ELSEVIER

Geomorphology 20 (1997) 49–65

GEOMORPHOLOGY

Avulsion and anastomosis in the panhandle region of the Okavango Fan, Botswana

Norman D. Smith [a,*], Terence S. McCarthy [b], W.N. Ellery [c], Charles L. Merry [d], Heinz Rüther [d]

[a] *Department of Geological Sciences (m / c 186), University of Illinois at Chicago, 845 West Taylor Street, Chicago, IL 60607, USA*
[b] *Department of Geology, University of the Witwatersrand, P.O. Wits, Johannesburg, 2050, South Africa*
[c] *Department of Geographical and Environmental Sciences, University of Natal, Durban, 4001, South Africa*
[d] *Department of Surveying and Geodetic Engineering, University of Cape Town, Private Bag, Rondebosch, 7700, South Africa*

Received 13 March 1996; revised 29 July 1996; accepted 19 November 1996

Abstract

GPS water-surface elevation data from the panhandle region of the Okavango Fan (northwestern Botswana) show that a prominent anastomosed reach occurs within a relative valley-gradient depression inferred to represent a small graben structure. The Okavango River undergoes an abrupt change in pattern as it approaches the upstream fault zone of the graben, developing small meander loops and higher sinuosity in response to increased valley slope induced by faulting. Four channels split from and ultimately rejoin the Okavango trunk channel to define the anastomosed reach. The oldest (Filipo channel) diverted from the Okavango on the upstream horst block, rejoining the trunk channel 26 km downstream within the graben. The younger channels B, C and D all developed subsequent to the Filipo avulsion by forming linkages between the Okavango trunk and floodplain tributaries that had evolved by headward extension and incorporation of older abandoned channel segments. Diversion of the three younger anastomosed channels was likely abetted by increased aggradation of the trunk channel following down-faulting. Neotectonic movement, although involving only slight displacement, is seen to be the underlying cause of avulsion, anastomosis, and certain channel pattern changes in the Okavango panhandle. This contrasts with other parts of the Okavango Fan system where avulsion appears to result more from autogenic in-channel sedimentation conditioned by various roles of vegetation.

Keywords: avulsion; Okavango River; anastomosing streams; fluvial sedimentation; neotectonics, geomorphologic effects; sinuosity

1. Introduction

Avulsion is a well-recognized feature of aggrading river systems and a fundamental process for building extensive alluvial deposits in floodplains. An avulsion diverts all or part of the discharge of a river to a lower part of the adjacent floodplain to form a new channel. Anastomosed channel networks may result in cases of multiple avulsions where the diverted flows rejoin downvalley. It is widely assumed that avulsions respond to gradient advantages created between channel and floodplain, and that the diverted flow will follow the direction of maximum slope away from the old channel. Less clear, however, are the mechanisms which govern the location and timing of avulsions, particularly the relative

* Corresponding author. Fax: +1 312 413-2279.

PII S0169-555X(96)00051-7

roles of differential aggradation and tectonic movement. Many avulsions in modern rivers appear to be explainable without direct recourse to tectonic causes (Speight, 1965; Smith and Smith, 1980; Smith, 1983; Wells and Dorr, 1987; Schumann, 1989; Smith et al., 1989; Brizga and Finlayson, 1990; Li and Finlayson, 1990; McCarthy et al., 1992; Richards et al., 1993; Blum, 1994; Tornqvist, 1994), but cases also occur in which avulsions have been attributed to tectonic movements (Coleman, 1969; Mike, 1975; McDougall, 1989; Blair and McPherson, 1994; Dumont, 1994; Harbor et al., 1994).

The Okavango Fan occupies a seismically active region of northern Botswana and is known to have experienced major flow diversions in historical times (Wilson, 1973; Shaw, 1984). Tectonic movements have been suggested as possible causes for these diversions (Wilson, 1973; Hutchins et al., 1976; Cooke, 1980), although direct evidence has been lacking. On the other hand, McCarthy et al. (1992) show that in at least one case, avulsion results from a series of feedback mechanisms driven primarily by channel aggradation. Although McCarthy et al. suggest that such channel sedimentation may be the cause of other Okavango avulsions, some linkage between avulsion and tectonic activity remains a distinct possibility in view of the evidence for other neotectonic influences on the geomorphology of the region (Cooke, 1980; Thomas and Shaw, 1991; McCarthy et al., 1993b).

To further address this question of neotectonics versus sedimentation as a cause of avulsion in the Okavango Fan, we examine here a portion of the fan system using Global Positioning System (GPS) elevation data. We focused on a region of the so-called 'panhandle' in which several flow diversions have created a widely spaced network of anastomosed channels, the most clearly defined region of anastomosis in the fan system. Although spatially accurate topographic maps are available for the Okavango region, elevations are not well constrained because of the paucity of survey reference points.

2. The Okavango Fan

The Okavango River is sourced mostly in central Angola and terminates in a broad flat plain in northwestern Botswana variously referred to as the Okavango Delta, Okavango Swamps, or more recently and our preference, Okavango Fan (Stanistreet and McCarthy, 1993a). One of the largest subaerial fans in the world, it extends some 150 km along radial axes and comprises about 22 000 km^2 of channels, lakes, islands, and seasonal and permanent wetlands (Fig. 1). Except for its marginal areas, the fan is virtually unpopulated and difficult to access. The catchment is mostly pristine and lacks major artificial structures which interfere with natural discharge variations.

The fan system is broadly divisible into three parts (Wilson, 1973): (1) an upper entry corridor, or panhandle, approximately 100 km long and 10 km wide; (2) a central zone of perennial swamps transected by several distributary channels confined by densely vegetated peat banks, and (3) a lower zone of seasonal swamps where peat is sparse or absent and flow is mostly unconfined. As it enters the panhandle, Okavango discharge averages approximately 335 m^3/s (Wilson and Dincer, 1976). Peak seasonal discharges (order 700 m^3/s) at the panhandle apex occur in February–March, then spread slowly through the swamplands, requiring about 4 months for a much-reduced flow peak to reach the distal margin of the fan. Approximately 95% of the total water budget, some 16 km^3 (discharge plus precipitation), is lost by evapotranspiration during its traverse over the fan surface, whereas the remainder escapes through groundwater and surface outflow (Dincer et al., 1981, 1987). All terrigenous influx is deposited on the fan surface which, together with significant subsurface precipitation of carbonate and silica in the lower fan region (McCarthy et al., 1993a), has resulted in approximately 300 m of total accumulation of probable Cenozoic age (Hutchins et al., 1976).

Active channels transport mainly moderately sorted medium and fine sand, with no obvious down-fan textural trends (Stanistreet and McCarthy, 1993a). A characteristic feature of the fan is its paucity of silt and clay-sized sediment, a consequence of its predominantly eolian sand provenance in the Kalahari Basin. Data from McCarthy and Metcalfe (1990) and McCarthy et al. (1991) suggest that only about 15% of the total terrigenous sediment input is suspended load. As a consequence, the fan generally lacks

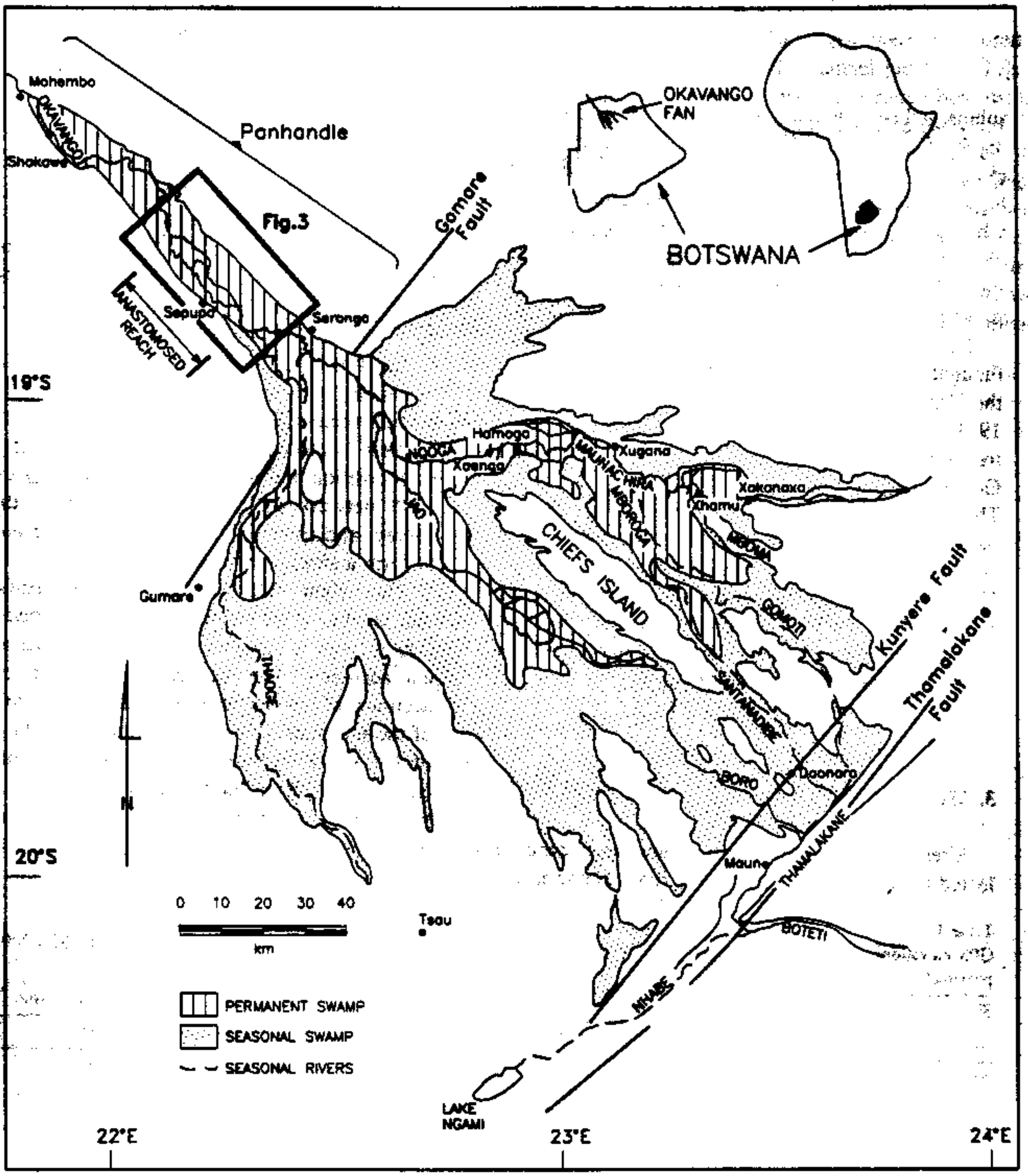

Fig. 1. Map showing locations of Okavango Fan, panhandle region, anastomosed reach, permanent and seasonal swamps, and major faults.

many features commonly associated with aggrading alluvial systems such as sediment-rich levees, crevasse splays, fine-grained cohesive banks, or mud-rich flood basins. Upper-fan and panhandle channels are bound by thick stands of papyrus (*Cyperus papyrus*, a large sedge) and to a lesser extent reed grasses *Phragmites australis* and *Miscanthus junceus*, all of which are rooted in porous submerged peat which commonly extends to the full depth of the channel (Ellery et al., 1989; McCarthy et al., 1991). These peat-plus-vegetation stands form highly resistant and well-defined channel margins which allow slow but free exchange of flow between channels and flanking swamplands. The porous nature of the channel margins prevent abrupt changes in water stages during seasonally variable discharges.

The Okavango Fan is set in a graben structure thought to represent the southwestern extension of the East African rift system (Fairhead and Girdler, 1971; Scholz et al., 1976). Three major northeast-trending faults confine most of the fan system: the Gomare fault on the northwest and the Kunyere and Thamalakane faults on the southeast (Fig. 1). The panhandle probably represents a smaller graben bound by northwesterly faults (McCarthy et al., 1993b). The region is seismically active (Reeves, 1972; Scholz et al., 1976), and satellite imagery reveals numerous lineaments of probable tectonic association (Hutchins et al., 1976; McCarthy et al., 1993b).

3. Methods

Sites for GPS elevation measurements were selected on elevated ground near active channels, usually abandoned termite mounds or small islands, and marked by embedding 1.5 m steel stakes. Using static differential methods (Cornelius et al., 1994), six sites in the panhandle were surveyed in 1994 (BPS 320, UCT 1–5) (Table 1). Because only two of these occurred in the anastomosed reach, 10 additional sites (UCT 13–22) were surveyed in September 1995 (Fig. 2). Five Ashtech M-12 receivers were used for the GPS survey, with observation sessions lasting 1 to 2 h. The carrier phase double-difference technique, with ambiguities fixed, was used to process all vectors. Redundant measurements were made to form a closed network, and the consistency in both position and height was better than 5 mm. The 1995 network included three points of the 1994 survey, and the combined networks were readjusted to form a single consistent network.

The height difference between GPS stations and the nearby water surface was determined with a digital level. Although the digital level had an inherent accuracy of a few millimeters, the estimated accuracy of this connection is about one cm because of the uncertainty in visually estimating the position of the water surface. The 1995 survey required 3 days to complete, during which water level fluctuations were negligibly small. The 1994 water levels were adjusted to the 1995 survey for consistency and ease of comparison.

Table 1
GPS elevation data for water surfaces. Sites on each main channel are listed in order of increasing distance from BPS 320, the mo
proximal site

Site	Channel	Latitude (south)			Longitude (east)			Water	Distance from BPS 320 (	
		deg	min	sec	deg	min	sec	elevation, m	Valley	Channel
BPS 320	Okavango	−18	21	56.880	21	50	43.282	991.40	0.0	0.0
UCT 1	Okavango	−18	27	29.551	22	2	1.100	987.45	0.0	0.0
UCT 18	Okavango	−18	33	10.832	22	6	18.290	985.46	25.0	37.3
UCT 2	Okavango	−18	35	39.372	22	7	7.156	984.67	37.5	63.5
UCT 17	Okavango	−18	39	1.186	22	7	14.470	983.23	41.7	71.5
UCT 16	Okavango	−18	40	55.484	22	10	20.413	981.90	47.7	85.8
UCT 15	Okavango	−18	41	56.527	22	10	14.065	981.65	54.3	100.5
UCT 3	Okavango	−18	44	40.570	22	11	48.256	980.64	55.3	102.3
UCT 14	Okavango	−18	45	36.739	22	13	4.730	980.06	61.9	115.5
UCT 13	Okavango	−18	47	59.790	22	15	31.880	978.98	64.7	122.5
UCT 4	Okavango	−18	48	57.167	22	17	22.407	978.68	70.9	137.5
UCT 5	Okavango	−18	49	14.354	22	24	57.945	977.00	74.9	142.5
UCT 19	Filipo	−18	37	15.709	22	9	36.972	983.21	87.1	167.5
UCT 20	Filipo	−18	39	10.708	22	11	25.951	981.64	46.2	80.3
UCT 21	Filipo	−18	41	34.113	22	11	37.579	980.78	52.2	92.5
UCT 22	Filipo	−18	43	49.106	22	14	50.700	979.96	56.4	102.1
									63.9	114.0

GPS provides differences of ellipsoidal height. For purposes of determining water-surface gradients, it is essential that the heights be referred to a level surface — the geoid. Geoidal corrections were obtained from a tailored geoid model (Merry, 1995) and applied to the data. The estimated relative accuracy of this model, based upon a comparison at three points of known geoidal height, is 3–4 cm, yielding a total estimated accuracy of about 5 cm for elevations of the water surface.

To assess the distribution of flow through the anastomosed reach, discharges were measured at cross-sections close to six channel junctions (Fig. 2). Velocity was measured from a tethered boat using a Watts current meter positioned successively at 0.5 m vertical intervals. Depending on channel width, 4 to 12 stations were occupied in a cross-section involving 14 to 55 individual velocity measurements. Mean velocity was computed by spatial integration of contoured flow fields and multiplied by channel cross-section area to give discharge. Cross-sections were chosen on relatively straight reaches approximately

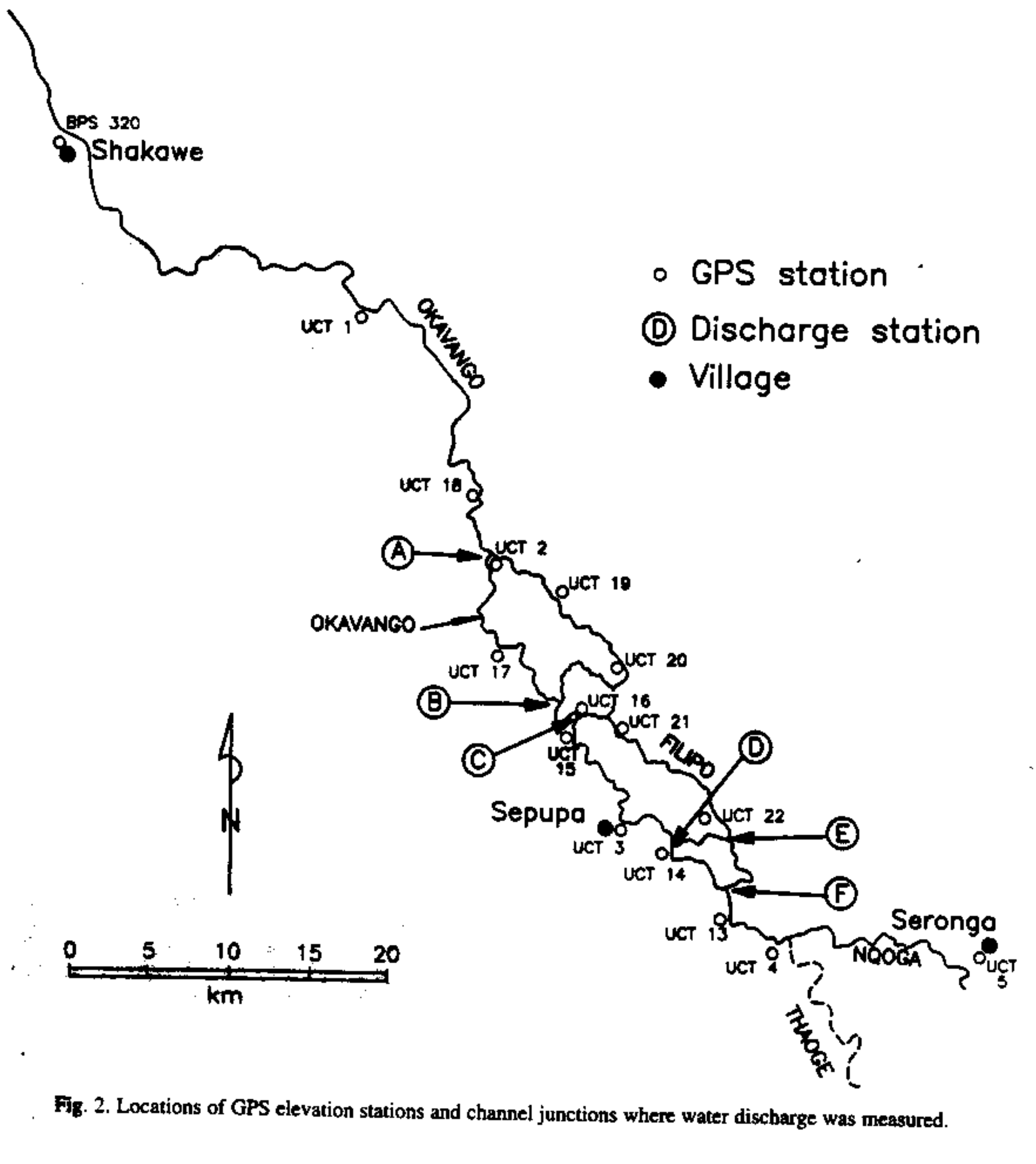

Fig. 2. Locations of GPS elevation stations and channel junctions where water discharge was measured.

100–200 m from the junctions. As each junction comprises three channel segments, only two discharges were measured directly and the third computed by difference. The accuracy of this method was justified at site D (Fig. 2) where all three channel segments were measured directly and shown to close within 2% of total discharge. Discharges were measured September 3–7, 1995, a period of gradually falling water levels from seasonal highs. Over the short interval of the survey, however, stage variations were negligible.

4. Results

4.1. Anastomosed reach

The anastomosed reach, fed by a single meandering channel, is 26 km long (straight-line) and occupies the lower middle portion of the panhandle. Below the anastomosed reach, the Okavango divides into the Nqoga and Thaoge channels, the latter which has become slowly abandoned since the late 1800s. The adjacent floodplain is covered by remnants of older meander belts of unknown ages (Fig. 3). Abandoned channel topography is probably more abundant than shown, but is obscured by dense vegetation, especially in areas flanking present channels (e.g., lower left portion of Fig. 3).

Four channels, the Filipo and three unnamed channels here referred to as 'B', 'C' and 'D', divert off and ultimately rejoin the Okavango trunk channel to comprise the anastomosed reach. The reach begins with the eastward diversion of the Filipo channel which rejoins the Okavango 23 km downvalley. Approximately 10 and 12 km downvalley from the Filipo diversion, respectively, the B and C channels divert eastward from the Okavango trunk to link with the Filipo. Further downstream, the D channel splits from the west side of the Okavango, rejoining it slightly downstream of the Filipo/Okavango conversion. The creation of the D channel resulted in a 6 km, or 45%, reduction in channel length for Okavango flow. Of the four avulsion channels, the D and Filipo channels draw the most flow from the Okavango trunk, followed by C, then B (Fig. 4, Table 2). Leakage through the porous margins of the channel occurs throughout the anastomosed reach, but is especially apparent between sites A and B (leakage into channel from adjacent swamps) and between sites E and F (leakage away from the trunk channel, partly recaptured by channel D) (Fig. 4). The slight overall gain in discharge through the anastomosed reach (A to F) represents net drawdown of flow out

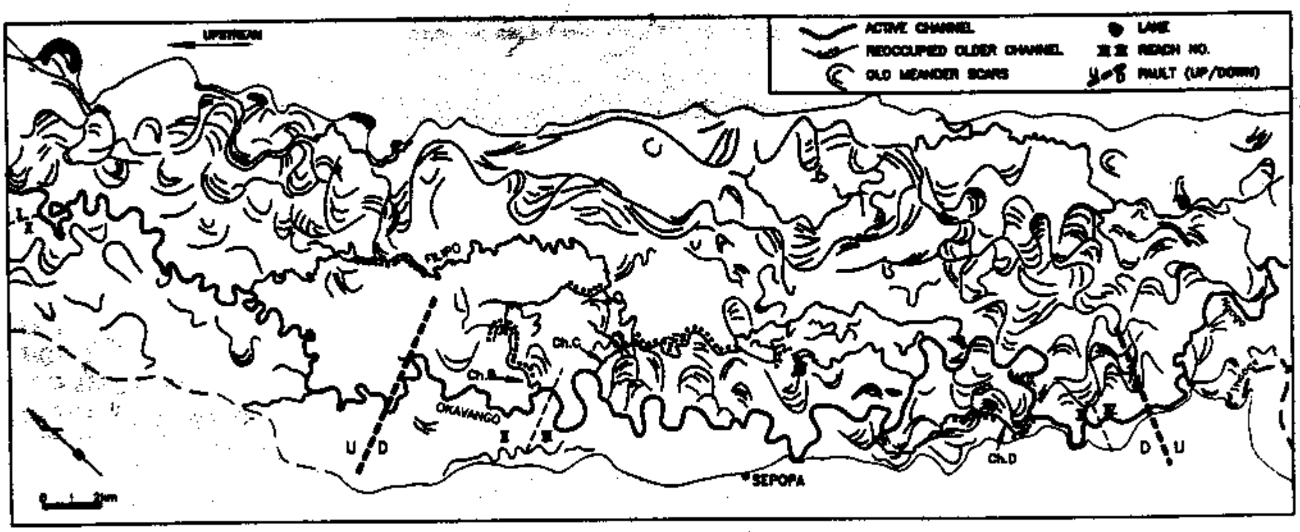

Fig. 3. Portion of panhandle showing main channels of present anastomosed reach and older channel topography in the floodplain. Portions of the floodplain surface are obscured by dense vegetation, especially along Okavango and upper Filipo channels. Reach numbers refer to Fig. 8. Heavy dashed lines show approximate positions of faults inferred from elevation data (Fig. 9) and discussed in text. Traced from 1:50000 aerial photographs.

of the flanking wetlands during declining phases of the seasonal discharge cycle.

The channels of the anastomosed reach are fairly uniform in depth and velocity despite an over 10-fold range in observed discharges (Table 2). Except for site F_3, which is an overfit older channel reoccupied by channel D (Fig. 3), mean velocities average 0.50 m/s and range between 0.38 and 0.61 m/s (sites E_1 and B_1). Mean depths range from 2.03 (A_3) to 4.48 m (E_3) and average 2.94 m. Most variation in discharge is manifested in width changes (range 10–60 m), a consequence of the dominating effects of vegetation in regulating the dynamics and dimensions of Okavango channels (McCarthy et al., 1991; Ellery et al., 1993).

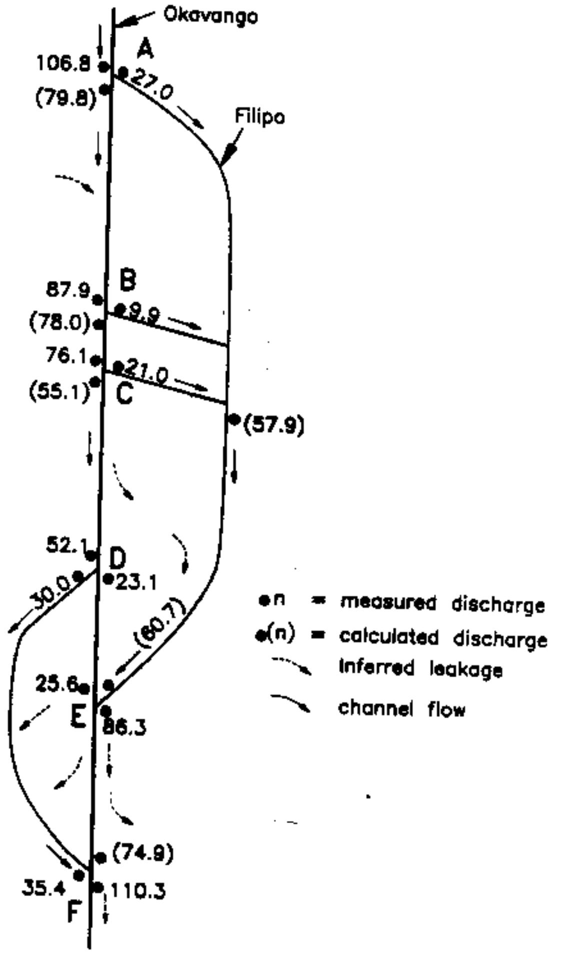

Fig. 4. Schematic depiction of water discharges through anastomosed reach September 3–7, 1995. The Okavango channel is arbitrarily shown as a straight line for illustration purposes. Lettered junctions correspond to locations in Fig. 2. Slight overall downstream increase in discharge (A to F) results from leakage into channels from flanking wetlands during declining phase of seasonal discharge cycle.

The development of anastomosis can be partially inferred from aerial photos, available for 1955 for the lower portions of the anastomosed reach, 1962 for the upper portions, and 1991 for the entire reach. The B and C channels formed after the Filipo was in place. In 1962, the B channel had two branches, each with a separate connection to the Filipo (Fig. 5A). The south branch probably formed entirely by headward extension from the Filipo, whereas the north branch incorporated segments of two abandoned channels. By 1991, all avulsive flow was confined to the north branch (Fig. 5B), suggesting that the south branch had formed first and was later captured by the north branch (the present B channel). The C channel formed after 1962 by linking the Okavango trunk to the lower part of the B-channel south branch by way of a small inactive and unconnected floodplain channel lying in wetlands just east of the Okavango (Fig. 5A,B). The upper portion of the C channel, i.e., the avulsive link to the Okavango, is nearly straight and probably formed quickly, perhaps by enlargement of a hippopatamus trail connecting the two channels (cf. McCarthy et al., 1992). Both the B and C avulsions occurred at the outer banks of meander bends, presumably because superelevation and higher flow velocities in bends are better able to test and exploit zones of weakness as potential avulsive connections to topographically lower floodplain areas.

Formation of the D channel followed a period of headward extension of a floodplain channel away from an older abandoned channel segment that intersected the Okavango at junction F (Fig. 6A). Avulsive linkage was made after 1955 where the floodplain channel closely approached a meander bend of the Okavango trunk channel (Fig. 6B). The flow diversion was artificially aided by activities of a local native group which sought to shorten the travel distance on the river between Sepupa and Seronga (Fig. 2) (P. Smith, pers. comm.). Growth of floodplain channels also can be observed between the Okavango and Filipo. These changes are partly attributed to increased flow in the Filipo following the C-channel avulsion, causing greater leakage out of the Filipo channel into its flanking wetlands and

Table 2
Channel data for six junctions in anastomosed reach. Locations shown in Fig. 2

Site	Description	Width, m	Depth, m	Velocity, m/s	W/D	Discharge, m^3/s
A_1	Okav. upstream	60	3.05	0.58	20	106.8
A_2	Okav. downstream	–	–	–	–	79.8 [a]
A_3	Filipo	28	2.03	0.48	14	27.0
B_1	Okav. upstream	54	2.66	0.61	20	87.9
B_2	Okav. downstream	–	–	–	–	78.0 [a]
B_3	Channel B	10	2.39	0.41	4	9.9
C_1	Okav. upstream	46	2.72	0.61	17	76.1
C_2	Okav. downstream	–	–	–	–	55.1 [a]
C_3	Channel C	12	3.38	0.52	4	21.0
D_1	Okav. upstream	34	2.75	0.56	12	52.1
D_2	Okav. downstream	24	2.09	0.46	12	23.1
D_3	Channel D	16	3.28	0.57	5	30.0
E_1	Okav. upstream	32	2.10	0.38	15	25.6
E_2	Okav. downstream	54	3.25	0.49	17	86.3
E_3	Filipo	28	4.48	0.48 [b]	6	60.7 [a]
F_1	Okav. upstream	–	–	–	–	74.9 [a]
F_2	Okav. downstream	56	3.61	0.55	16	110.3
F_3	Channel D	41	3.35	0.26	12	35.4

[a] Discharge calculated by difference.
[b] Width and depth measured; velocity calculated from discharge/(width × depth).

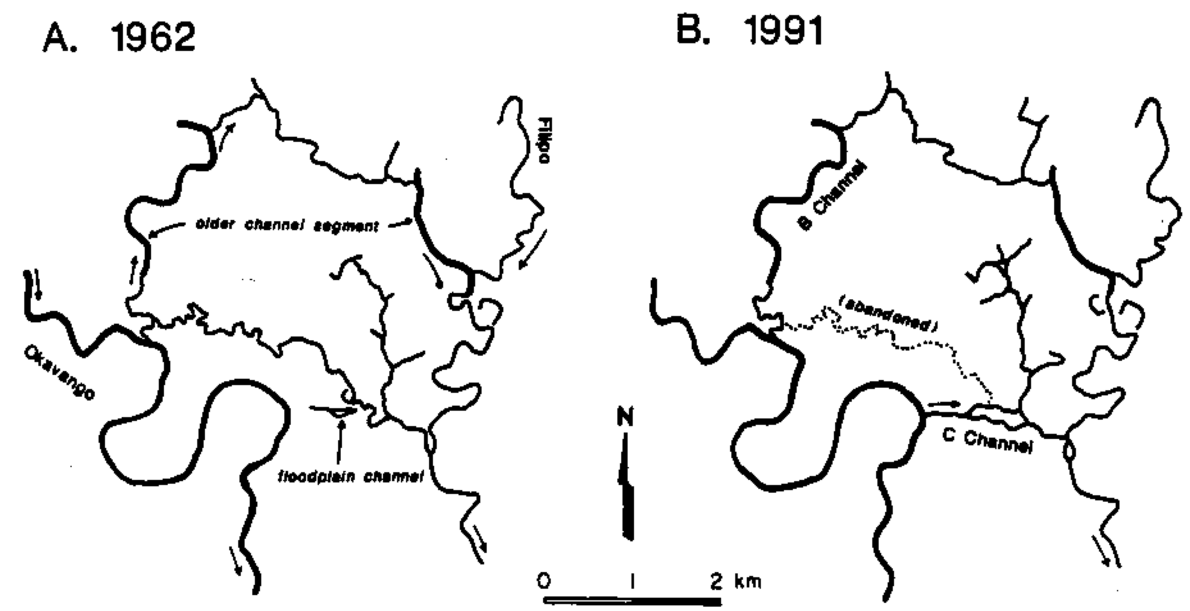

Fig. 5. Development of B and C channels. (A) In 1962, the B channel had two active branches connecting the Okavango and Filipo channels, with the northern branch comprising linked segments of two older channels. Both branches formed from Filipo tributaries after the Filipo was in place. (B) By 1991, south branch of B channel has abandoned, and C channel has formed by avulsive linkage with small floodplain channel segment, connecting Okavango with Filipo channel.

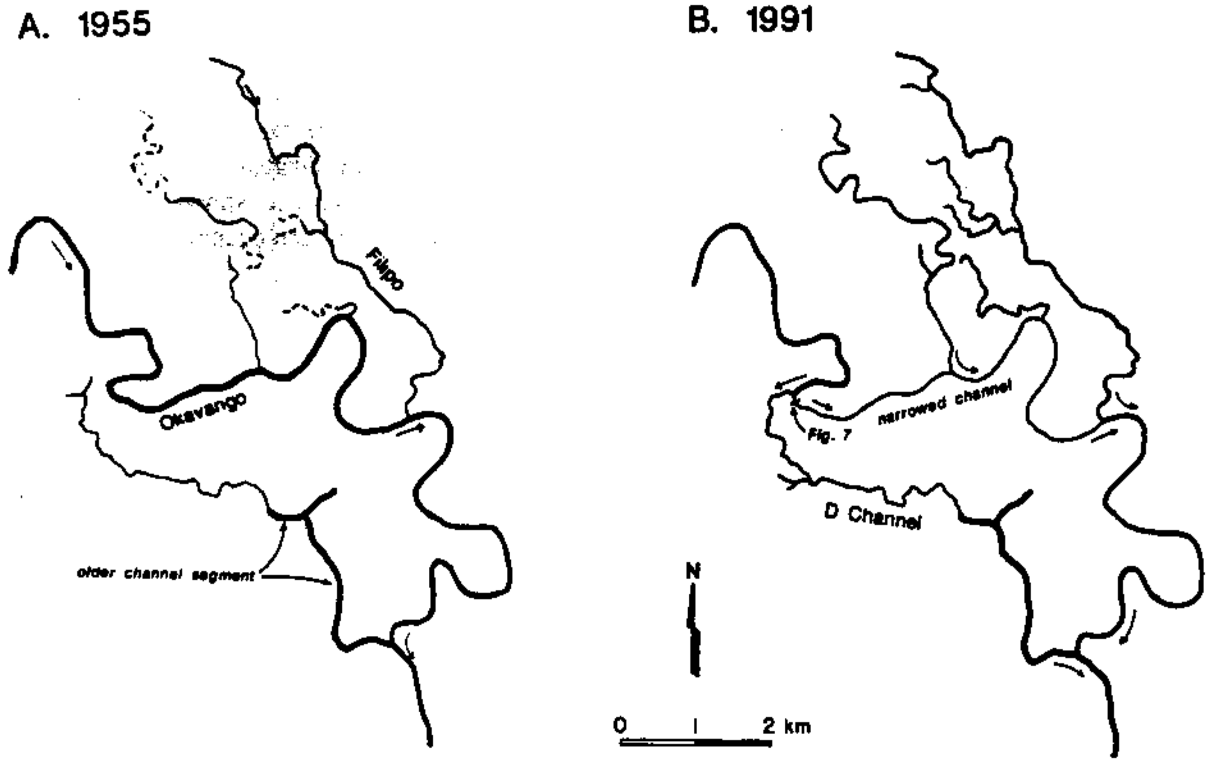

Fig. 6. Formation of D channel. (A) Tributary, after incorporating abandoned segment of older floodplain channel, moves headward to point near meander bend of Okavango channel. (B) Aided by human activities, the tributary joins with Okavango trunk to form D channel, followed by narrowing of Okavango channel immediately downstream from new junction (see Fig. 7). Added development of floodplain tributaries between Okavango and Filipo channels after 1955 are probably the result of increased Filipo discharge following formation of C channel upstream.

subsequently greater runoff from the wetlands back into the Okavango.

Following the formation of an avulsive channel, the trunk channel downstream from the new junction adjusts quickly to the resulting lowered discharge. This is most obviously manifested in width reduction by the dense and quickly growing stands of bank vegetation (Fig. 7).

4.2. Okavango channel pattern

Within and near the anastomosed reach, the Okavango trunk channel presently comprises four distinct reaches defined by meander patterns (Fig. 8). For each reach, sinuosity, p, mean radius of meander loop curvature, r (Brice, 1974), and standard deviation of loop curvature, σ, were computed from

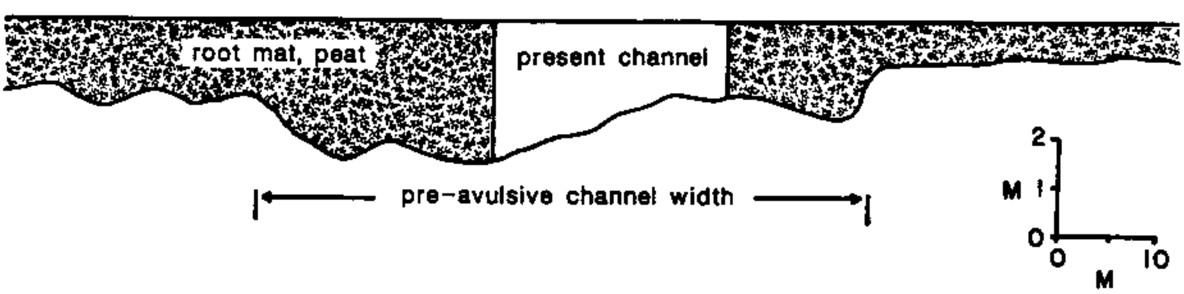

Fig. 7. Cross-section of Okavango channel 100 m downstream from junction D (Fig. 2). Channel margins, defined by dense vegetation and peat, have narrowed as a consequence of upstream flow diversions.

1 : 50 000 topographic maps. Reach I lies upstream of the anastomosed reach and is characterized by moderate sinuosity and broad open meander loops (p = 1.80, r = 463 m, σ = 178 m). Reach I passes abruptly into Reach II which overlaps into the anastomosed reach and features higher sinuosity (p = 2.36) and much smaller meander loops (r = 160 m, σ = 82 m). High sinuosity is maintained in Reach III (p = 2.35), but meander sizes are intermediate between those of Reaches I and II (r = 280 m, σ = 142 m). Reach IV (p = 1.90), lying downstream of the anastomosed reach, begins as a relatively straight channel connecting Reach III. Below the junction with the mostly abandoned Thaoge channel, the trunk channel (here called the Nqoga) comprises irregular and mainly small meanders (r = 167 m, σ = 106 m).

4.3. Water-surface elevation

GPS water-surface elevations for 16 sites along the Okavango and Filipo channels are given in Table 1, together with valley and channel distances as measured from BPS 320, the most proximal panhandle site. The plot of Okavango elevations against straight-line valley distance shows an abrupt mid-valley slope increase which occurs within the anastomosed reach between 42 and 54 km downstream of BPS 320 (Fig. 9). This plot removes the effect of channel sinuosity and approximates the profile of the floodplain or valley floor. Eleven of the 12 Okavango points can be closely fitted to three straight lines that, when extended, show vertical offsets of about 0.7 m between the upper and middle segments and 0.2 m between middle and lower segments 71–75 km downvally distance. The twelfth point falls in the offset zone between the upper and middle segments. In contrast, the four Filipo elevations define a slightly concave-up and topographically lower valley floor. When elevations of the Okavango channel are plotted against channel distance, i.e., sinuosity effects are restored, slope changes are less abrupt and appear to be defined by five straight-line segments (Fig. 10), four of which (**b**–**e**, Fig. 10) correspond approximately to the positions of Reaches I-IV within the constraints imposed by the locations of survey sites. Segment **a**, the most proximal and steepest ($s = 1.06 \times 10^{-4}$), is defined by only two points and is constrained by survey site positions to overlap Reach I. Most of Reach I, however, corresponds to segment **b** with its lower slope ($s = 0.76 \times 10^{-4}$) compared to segment **a**. Reach II indicates relative steepening (segment **c**, $s = 0.96 \times 10^{-4}$), and Reaches III and IV show successive reductions in channel slope (segment **d**, $s = 0.79 \times 10^{-4}$; segment **e**, $s = 0.66 \times 10^{-4}$). As in Fig. 9, water-surface elevations of the Filipo channel indicate a gentle concave profile lying topographically lower than the Okavango.

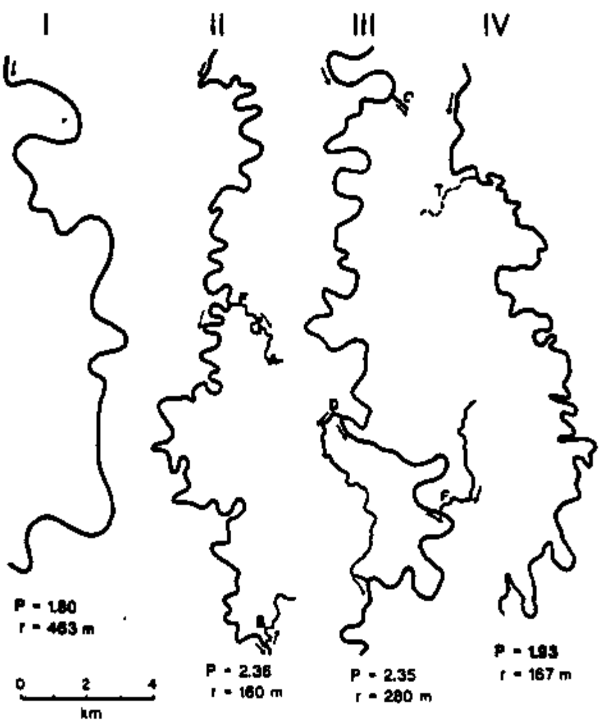

Fig. 8. Okavango Reaches I–IV as characterized by sinuosity (p) and radius of curvature (r). Linking channels: F = Filipo channel; B = B channel; C = C channel; D = D channel; T = Thaoge channel. Reaches are continuous from upstream (I) to downstream (IV). See Fig. 3.

Water-surface slopes for various channel segments of the anastomosed reach were calculated between selected survey points, in some cases involving interpolated elevations where survey points were located far from junctions (Fig. 11). For channels B, C and D, the slopes represent average values of entire lengths and, thus, probably underestimate proximal slopes near the diversions from the topographically higher Okavango channel. Although the Filipo shows a progressive downstream decline in channel slope, its proximal value probably also un-

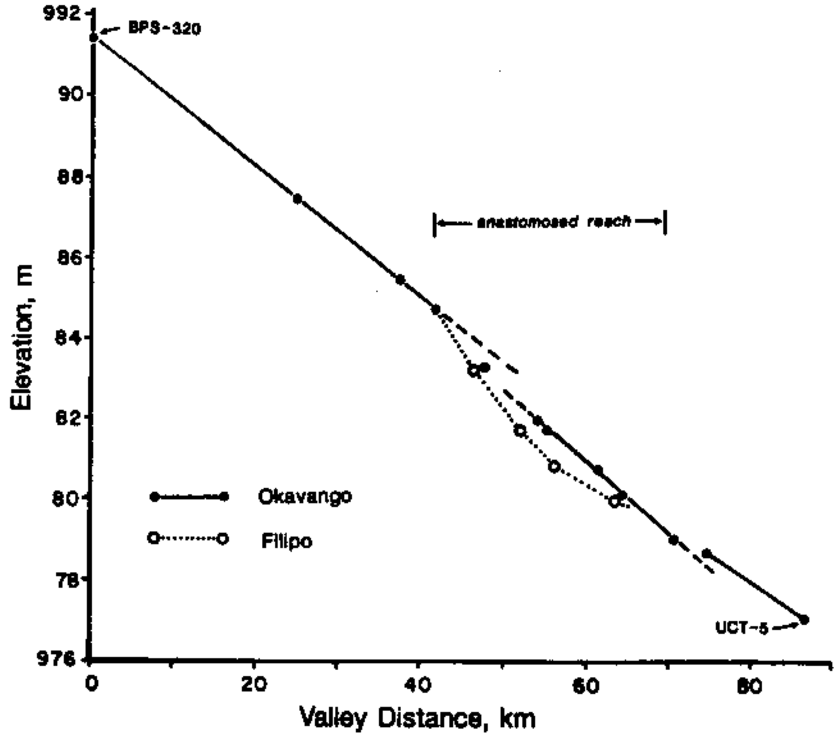

Fig. 9. Elevations of water surface of Okavango and Filipo channels versus straight-line valley distance. Sites BPS-320 and UCT-5 are indentified for ease of reference (Table 1). Dashed line extensions are included to show vertical offsets of three slope segments. Anastomosed reach occupies most of downwardly offset segment, interpreted as a small graben.

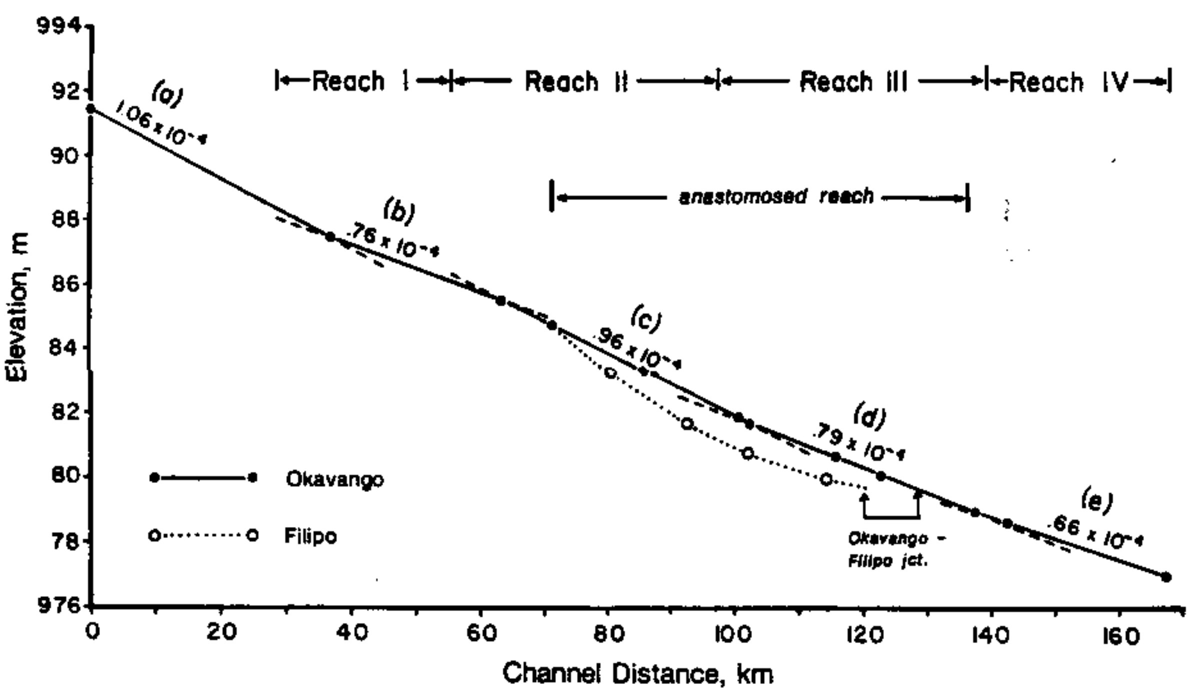

Fig. 10. Elevations of water surface versus channel distance. Five slope segments (a–e) are apparent for the Okavango, with the lower four approximately corresponding to Reaches I–IV (Fig. 8). Numbers indicate slope values for each Okavango segment. The downstream Okavango-Filipo junction does not close on a point because of differing sinuosities between the two channels.

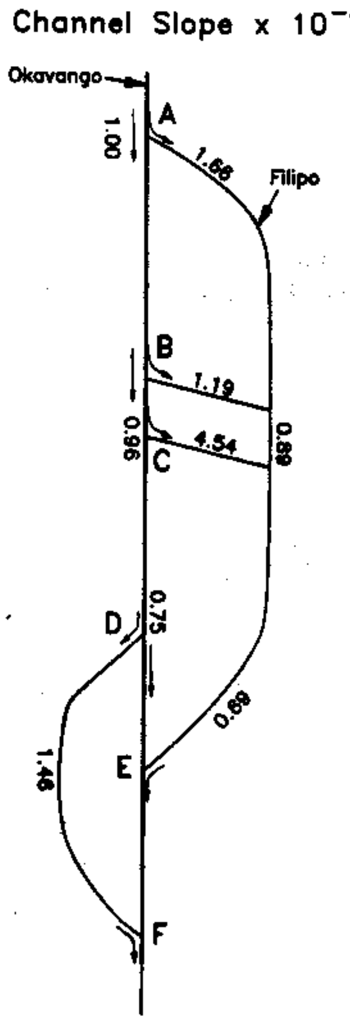

Fig. 11. Schematic depiction of water-surface slopes of different channel segments in the anastomosed reach. Slopes of divergent channels all exceed that of the Okavango trunk. Letters identify junctions (Fig. 2).

derestimates the actual slope close to the Okavango because of the large distance between survey points. Nevertheless, the slopes of all four diverted channels clearly exceed those of the contiguous Okavango trunk segments and thus represent gradient advantages for avulsion. For channel C, the shortest and straightest of the four (Fig. 3), the present gradient advantage (= slope of diverted channel/slope of trunk channel) is 4.7, whereas the other three range from 1.2 to 1.9. The lower values for the B, D and Filipo channels likely result from their greater lengths (greater distance between survey posts) and incorporation of older channel segments whose slopes approximate regional floodplain gradients.

5. Discussion

The abrupt downvalley change in elevations of the Okavango water surface between 42 and 54 km downvalley from BPS 320 (Fig. 9) is interpreted as offset by a small fault downthrown to the southeast. The smaller offset between 71 and 75 km is also interpreted as a fault displacement, which suggests that the anastomosed reach represented by the middle segment in Fig. 9 occurs in a small graben. A fault-block origin is reasonable in view of the seismic activity (Scholz et al., 1976), known major faults (Fig. 1), and abundant lineaments of presumed tectonic association (Hutchins et al., 1976; McCarthy et al., 1993b) that occur in the region. Interpretation as a fault block is preferred to one of simple downwarping because the structural style for the region is predominantly extensional (McCarthy et al., 1993b). Aerial photographs and Landsat imagery suggest that at least two possible lineaments, manifested as subtly aligned topographic elements, exist within the inferred upstream fault zone. Two other lineaments indentified by Hutchins et al. (1976) lie just outside the panhandle and when extended, project into the same zone. Nevertheless, surface expression of faulting is faint at best, and from available imagery we are unable to precisely place either fault with confidence. This could be attributed to its small or gradual displacement, the possibility of even smaller multiple faults, or the obscuring effects of dense vegetation. Approximate locations of the two inferred faults, however, are shown in Fig. 3.

The major break in slope in the Okavango downvalley profile (Fig. 9) is less apparent in the downchannel profile (Fig. 10) largely because of the sinuosity increase from Reach I to II (Fig. 8). The uppermost reach of the Okavango (segment **a**, Fig. 10) shows a slightly greater channel slope than the rest of the panhandle. This reach is consistently wider and less sinuous than the more intermediate and distal panhandle channels, in places exceeding 100 m (Wilson, 1973), which likely results in higher width-depth ratios as well. A single width-depth ratio of 27.9 was reported by McCarthy et al. (1991) near Shakawe compared to a range of 12 to 20 for Okavango channels in the anastomosed reach (Table 2). We infer that greater width-depth ratios in the most proximal reach (segment **a**) result in larger friction factors which in turn require a higher channel slope. We do not have data that permits an explanation for greater width/depth ratios in the most proximal reach.

The striking and abrupt pattern change between Reaches I and II represents a large decrease in the size of meander loops and a moderate increase in sinuosity. In the absence of accompanying discharge reduction or apparent changes in bank or bed material between the two reaches, the increased sinuosity in Reach II likely represents an adjustment toward decreasing channel slope to compensate for increased valley slope caused by fault displacement. Similar sinuosity adjustments to neotectonically induced changes in slope have been observed in other rivers as well (Welch, 1973; Adams, 1980; Burnett and Schumm, 1983; Ouchi, 1985; Harbor et al., 1994), though rarely so abruptly as shown between Reaches I and II. Diversion of flow to the Filipo has had little apparent effect on the character of Reach II (Fig. 8), which suggests that the development of small meanders and increased sinuosity in the Okavango trunk may post-date the Filipo avulsion. The relationship between the two events, however, is not clear. The small meanders in Reach II are atypical for the Okavango panhandle, either when compared to present contiguous reaches (I and III) or to older meander belts preserved in the floodplain (Fig. 3). Reach II is, therefore, interpreted as having a recently developed character that may be still adjusting to tectonic displacement. Its channel slope (segment **c**, Fig. 10), is still higher than adjoining reaches (segments **b**, **d**), and its unusually small meanders may be an adjustment for increasing friction within the channel in order to maintain a higher slope.

Reach III is believed to represent a largely undisturbed meander pattern typical of the lower half of the panhandle. Its present meander loops are similar in size to those of nearby abandoned meander belts (Fig. 3, note especially near Sepupa). Except for some narrowing (Fig. 7), the channel has not yet adjusted significantly to upstream avulsions (B, C, Filipo channels) which now draw approximately half of the flow out of the Okavango (Fig. 4). Prior to faulting, Reach I probably graded downstream into Reach III. The larger meanders of Reach I can be attributed to the higher discharges that characterize upper-panhandle channels, especially during rising and peak flows (Wilson and Dincer, 1976; McCarthy et al., 1991).

Downstream of the anastomosed reach, the Thaoge was the dominant channel until the late 1800s, when it began to abandon and avulse into the Nqoga, where virtually all flow is carried today. The small loops and irregular meander patterns of Reach IV (mainly the Nqoga) are interpreted as incomplete adjustments to the discharge inherited from the Thaoge. The relatively straight 3 km channel segment connecting Reaches III and IV (Fig. 8) crosses the downstream edge of the graben inferred in Fig. 9. Its low sinuosity is likely an adjustment to the lowered local valley slope imposed by the downstream horst block (cf. Schumm, 1993).

Directly after faulting, Reach II likely extended both headward and toeward from the trace zone of the upstream fault, involving dissection of the upthrown block and aggradation on the downthrown block. Such extension in both upstream and downstream directions may explain the abrupt transitions between Reaches I–II and II–III (Fig. 8). The Filipo avulsion originated on the upthrown block, possibly by a mechanism proposed by Mackey and Bridge (1995) in which up-block avulsion is initiated by an increasing ratio of cross-valley (away from channel) to down-valley slope as a consequence of relative movements along the fault plane. The new Filipo channel extended downvalley across the fault and parallel to the Okavango trunk, reoccupying at least two segments of older abandoned channels before rejoining the Okavango (Fig. 3). Prior to avulsion, the Okavango likely flowed on a slightly elevated alluvial ridge composed of peat and dense vegetation, similar to other areas of the modern fan system (Ellery et al., 1993; Stanistreet et al., 1993b). Faulting and subsequent downvalley extension of Reach II, together with slope reduction caused by the downstream graben fault, caused further aggradation which eventually resulted in a present maximum difference in elevation of about one meter between the mid-reach Filipo and Okavango (Fig. 10). Once the Filipo channel was in place, it began to form its own floodplain tributaries which lengthened headward in time and incorporated older abandoned channel segments wherever encountered. Such abandoned channelways are abundant in the Okavango fan system because of the paucity of suspended detrital sediment which permits them to remain unplugged for long periods. Headward extension of Filipo tributaries eventually intersected the Okavango trunk to form connecting channels B and C. Channel D, although part of the anastomosed reach, represents channel self-shortening and does not appear to be related to the upstream fault or to the Filipo avulsion. It occurs entirely within the graben, however, and its origin may be attributable in part to increased aggradation of the Okavango trunk channel following faulting, particularly the damming effect of the downstream horst.

The amount of fault displacement cannot be precisely determined because the present elevation offset (Fig. 9) reflects both faulting and subsequent but unknown amounts of deposition on the downthrown block. The present 0.7 m offset represents a minimum value of fault displacement assuming zero subsequent aggradation and all channel-slope adjustments assumed by sinuosity changes. Development of the B and C channels, linking the higher Okavango with the lower-elevation Filipo mid-reach, suggests the Filipo has not yet developed an alluvial ridge, which in turn implies minimal Filipo aggradation. Elevation of Filipo mid-reaches (52–57 km, Fig. 9) could, therefore, be taken as approximating the pre-aggradation surface of the downthrown block after faulting, giving a displacement of about 1.5 m (Fig. 9). Given the uncertainties of dealing with such small elevation differences, we estimate fault displacement to have been about one meter. The age of the fault is not known, but given the relatively undramatic changes in the Filipo and the fault-induced Reach II since 1955, we estimate that faulting occurred (or began) in the order of several decades to centuries earlier.

The scenario for avulsion and anastomosis interpreted here for the panhandle differs significantly from that of McCarthy et al. (1992) for the main Okavango fan, where avulsion is seen to result entirely from autogenic sedimentation processes and conditioned by various roles of vegetation. There, avulsion results from progressive and gradual displacement of flow to adjacent swamplands forced by channel-bed aggradation. Linkage to an adjacent but separately developing floodplain channel is later made through some existing line of weakness, commonly a hippopotamus trail, which then enlarges to eventually draw off remaining flow from the failing trunk channel to complete the avulsion. The Nqoga channel probably developed from the now-defunct Thaoge in this manner (Wilson, 1973). Anastomosed channels B, C and D are similar in that they resulted from linkages of separately developed floodplain channels to the Okavango trunk, possibly also involving hippopotamus trails as final connections (though this cannot be demonstrated). None of these avulsions, however, involved prior aggradation and failure of a trunk channel immediately downstream of its avulsive junction as described by McCarthy et al. (1992). Moreover, all of the involved channel segments retained significant portions of total discharge, thus creating the present anastomosed network. The underlying difference between the two situations is the effect of panhandle neotectonics in which avulsion, aggradation, and anastomosis are all linked to a small graben structure.

Given the potential importance of the Okavango as a regional water resource (Wilson and Dincer, 1976) and the close relationship between panhandle communities and channel positions, it may be useful to speculate on the longer term outcome of the present evolutionary trends involving the anastomosed reach. Judging from the abundance of abandoned meander belts (Fig. 3), the panhandle has experienced repeated shifts of channel position in the past, and probably will continue to do so in the future. The relatively recent (post-1950s) changes in the channel network, including headward extension of floodplain channels, abandonment of the B-channel south branch, and creation of the C and D channels, suggest the anastomosed reach is still in a stage of rapid modification evolving toward some new state of dynamic equilibrium. Relatively higher rates of alluvial deposition could be expected in the anastomosed network because this reach occurs mostly within the topographically lower fault graben. This is supported by earlier bedload measurements at sites above and below the anastomosed reach (McCarthy et al., 1991, Table 1; their locs. 'I' and 'H' which approximately correspond to sites UCT-1 and UCT-4, respectively; see Fig. 2). Two sets of measurements, taken 16 months apart, showed 5-fold and 2-fold reductions in bedload transport between upstream and downstream stations, suggesting net channel aggradation within the anastomosed reach.

Most of this aggradation probably occurs in the upper reaches of the Filipo and the lower portion of Reach II, the latter in association with its downstream extension away from the fault. As long as such channel aggradation continues, thereby increasing elevation differences between the channel and its adjoining floodbasin, additional flow diversions are likely and a multi-channel network will be maintained. As new anastomosing channels develop by avulsion, however, older ones will become abandoned as flow and sediment are diverted into lower areas of the surrounding wetlands. Slow abandonment appears to be underway now in the Okavango channel segment between sites D and E (Figs. 2 and 7) in response to the recent D-channel diversion. Likewise, the small discharge and low slope advantage of the B channel (Figs. 4 and 11) possibly portends its imminent abandonment, particularly since the upper Filipo (i.e., the B-channel base level) is likely aggrading (see above). As flow, sediment movement, and channel patterns continue to adjust to the perturbation in floodplain gradient caused by faulting, the long-term fate of the anastomosed reach will likely be reversion to a single dominant meandering channel (cf. Smith et al., 1989). Given its present favorable position in a low part of the floodplain, the Filipo would appear to be the most likely eventual position of the Okavango for this portion of the panhandle.

6. Conclusions

Precise GPS elevation data in the Okavango panhandle, accurate to within 5 cm, indicates a relative depression in the downvalley profile of the water surface which we interpret to represent a small graben bound by minor low-displacement faults. The graben contains a well-defined anastomosed reach and abrupt transitions in the meander patterns of the main trunk channel. Reach II, characterized by high sinuosity and anomalously small meander loops, overlaps the upstream bounding fault and is seen to represent adjustment to the abrupt local increase in slope imposed by faulting. The Filipo channel avulsed from the Okavango on the upthrown block, rejoining the trunk channel within the graben and later forming two additional linkages to the Okavango (channels B and C) by connections with floodplain tributaries. Channel D, also part of the anastomosed network, represents shortening of the main trunk; it formed, assisted by human activity, following headward extension of a floodplain channel, but was probably aided by aggradation forced by the damming effect of the small downstream fault. All four avulsions are incomplete, i.e., significant discharge has remained in the affected trunk channel so that the reach could develop its present anastomosing character.

Avulsion, anastomosis, and channel-pattern changes in the mid-panhandle reach are direct consequences of localized neotectonic movement. Vertical displacement of the graben was probably minor (order 1 m), and its presence could not have been inferred without the assistance of GPS elevation data, despite the unusual character of this reach compared to the rest of the Okavango fan system. Anomalous channel patterns elsewhere may be similarly interpretable from the highly accurate elevation data obtainable from differential GPS techniques.

Acknowledgements

The authors thank Dion Brandt, Mike Berry, Walter Volkman, Hans Heister and Armin Grun for technical support in the field; Mike Bullock for boats; and Judy Wilmot, Di Du Toit and Lyn Whitfield for assistance with manuscipt preparation. Financial support was provided by the Foundation for Research Development, the Universities of Cape Town and the Witwatersrand, and for the first author, US National Science Foundation Grant EAR-9304104.

References

Adams, J., 1980. Active tilting of the United States midcontinent: geodetic and geomorphic evidence. Geology, 8: 442–446.

Blum, M.D., 1994. Genesis and architecture of incised valley fill sequences: a Late Quaternary example from the Colorado River, Gulf Coastal Plain of Texas. In: P. Weimer and H.W. Posamentier (Editors), Siliciclastic Sequence Stratigraphy: Recent Developments and Applications. Am. Assoc. Petrol. Geol. Mem. 58, pp. 259–283.

Blair, T.C. and McPherson, J.G., 1994. Historical adjustments by

Walker River to lake-level fall over a tectonically tilted half-graben floor, Walker Lake Basin, Nevada. Sediment. Geol., 92: 7–16.

Brizga, S.O. and Finlayson, B.L., 1990. Channel avulsion and river metamorphosis: the case of the Thompson River, Victoria, Australia. Earth Surf. Process. Landforms, 15: 391–404.

Brice, J.C., 1974. Evolution of meander loops. Geol. Soc. Am. Bull., 85: 581–586.

Burnett, A.W. and Schumm, S.A., 1983. Alluvial-river response to neotectonic deformation in Louisiana and Mississippi. Science, 222: 49–50.

Coleman, J.F., 1969. Brahmaputra River: channel process and sedimentation. Sediment. Geol., 3: 131–239.

Cooke, H.J., 1980. Landform evolution in the context of climatic change and neo-tectonism in the Middle Kalahari of north-central Botswana. Trans. Inst. Br. Geogr., New Ser., 5: 80–99.

Cornelius, S.C., Sear, D.A., Carver, S.J. and Heywood, D.I., 1994. GPS, GIS, and geomorphological field work. Earth Surf. Process. Landforms, 19: 777–787.

Dincer, T., Hutton, L.G. and Khupe, B.B.J., 1981. Study, using stable isotopes of flow distribution, surface-groundwater relations and evapotranspiration in the Okavango Delta, Botswana. Intern. Atomic Energy Agency Proc., Ser. SII/AUB 493, pp. 3–26.

Dincer, T., Child, S. and Khupe, B.B.J., 1987. A simple mathematical model of a complex hydrologic system, Okavango Swamp, Botswana. J. Hydrol., 93: 41–65.

Dumont, J.F., 1994. Neotectonics and rivers of the Amazon headwaters. In: S.A. Schumm and B.R. Winkley (Editors), The Variablilty of Large Alluvial Rivers. A.S.C.E. Press, New York, pp. 103–113.

Ellery, W.N., Ellery, K., McCarthy, T.S., Cairncross, B. and Oelofse, R., 1989. A peat fire in the Okavango Delta, Botswana, and its importance as an ecosystem process. Afr. J. Ecol., 27: 7–21.

Ellery, W.N., Ellery, K., Rogers, K.H., McCarthy, T.S. and Walker, B.H., 1993. Vegetation, hydrology, and sedimentation processes as determinants of channel form and dynamics in the northeastern Okavango Delta, Botswana. Afr. J. Ecol., 31: 10–25.

Fairhead, J.D. and Girdler, R.W., 1971. The seismicity of Africa. Geophys. J. R. Astronom. Soc., 24: 271–301.

Harbor, D.J., Schumm, S.A. and Harvey, M.D., 1994. Tectonic control of the Indus River in Sindh, Pakistan. In: S.A. Schumm and B.R. Winkley (Editors), The Variability of Large Alluvial Rivers. A.S.C.E. Press, New York, pp. 161–175.

Hutchins, D.G., Hutton, L.G., Hutton, S.M., Jones, C.R. and Loenhert, E.P., 1976. A summary of the geology, seismicity, geomorphology, and hydrogeology of the Okavango Delta. Geol. Surv. Botswana, Bull., 7, pp. 1–27.

Li, S. and Finlayson, B.L., 1990. Flood management of the lower Yellow River: hydrological and geomorphological perspectives. Sediment. Geol., 85: 285–296.

Mackey, S.D. and Bridge, J.S., 1995. Three-dimensional model of alluvial stratigraphy: theory and application. J. Sediment. Res., B65: 7–31.

McCarthy, T.S. and Metcalfe, 1990. Chemical sedimentation in the semi-arid environment of the Okavango Delta, Botswana. Chem. Geol., 89: 157–178.

McCarthy, T.S., Stanistreet, I.G. and Cairncross, B., 1991. The sedimentary dynamics of active fluvial channels on the Okavango fan, Botswana. Sedimentology, 38: 471–487.

McCarthy, T.S., Ellery, W.N. and Stanistreet, I.G., 1992. Avulsion mechanisms on the Okavango fan, Botswana: the control of a fluvial system by vegetation. Sedimentology, 39: 779–795.

McCarthy, T.S., Ellery, W.N. and Ellery, K., 1993a. Vegetation-induced subsurface precipitation of carbonate as an aggradational process in the permanent swamps of the Okavango (delta) fan, Botswana. Chem. Geol., 107: 111–131.

McCarthy, T.S., Green, R.W. and Franey, N.G., 1993b. The influence of neo-tectonics on water dispersal in the northeastern regions of the Okavango swamps, Botswana. J. Afr. Earth Sci., 17: 23–32.

McDougall, J.W., 1989. Tectonically induced diversion of the Indus River west of the Salt Range, Pakistan. Palaeogeogr., Palaeoclimatol., Palaeoecol., 71: 301–307.

Merry, C.L., 1995. A local geoid model for the Okavango Delta. Intern. Union Geodesy and Geophys. XXI Gen. Assem., Boulder, CO., USA.

Mike, K., 1975. Utilization of the analysis of ancient river beds for the detection of Holocene crustal movements. Tectonophysics, 29: 359–368.

Ouchi, S., 1985. Response of alluvial rivers to slow active tectonic movement. Geol. Soc. Am. Bull., 96: 504–515.

Reeves, C.V., 1972. Rifting in the Kalahari? Nature, 237: 95–96.

Richards, K., Shobhit, C. and Friend, P., 1993. Avulsive channel systems: characteristics and examples. In: J.L. Best and C.S. Bristow (Editors), Braided Rivers. Geol. Soc. Spec. Publ., 75, pp. 195–203.

Scholz, C.H., Koczynski, T.A. and Hutchins, D.G., 1976. Evidence for incipient rifting in southern Africa. Geophys. J. R. Astronom. Soc., 44: 135–144.

Schumann, R.R., 1989. Morphology of Red Creek, Wyoming, an arid-region anastomosing channel system. Earth Surf. Process. Landforms, 14: 277–288.

Schumm, S.A., 1993. River response to baselevel change: implications for sequence stratigraphy. J. Geol., 101: 279–294.

Shaw, P.A., 1984. A historical note on the outflows of the Okavango Delta system. Botswana Notes and Records, 16: 127–130.

Smith, D.G., 1983. Anastomosed fluvial deposits: modern examples from western Canada. In: J.D. Collinson and J. Lewin (Editors), Modern and Ancient Fluvial Systems, Intern. Assoc. Sediment. Spec. Publ. 6, pp. 155–168.

Smith, D.G. and Smith, N.D., 1980. Sedimentation in anastomosed river systems: examples from alluvial valleys near Banff, Alberta. J. Sediment. Petrol., 50: 157–164.

Smith, N.D., Cross, T.A., Dufficy, J.P. and Clough, S.R., 1989. Anatomy of an avulsion. Sedimentology, 36: 1–23.

Speight, J.G., 1965. Flow and channel characteristics of the Angabunga River, Papua. J. Hydrol., 3: 16–36.

Stanistreet, I.G. and McCarthy, T.S., 1993a. The Okavango Fan and the classification of subaerial fan systems. Sediment. Geol., 85: 115–133.

Stanistreet, I.G., Cairncross, B. and McCarthy, T.S., 1993b. Low sinuosity and meandering bedload rivers of the Okavango Fan: channel confinement by vegetated levees without fine sediment. Sediment. Geol., 85: 135–156.

Thomas, D.S.G. and Shaw, P.A., 1991. The Kalahari Environment. Cambridge Univ. Press, pp. 284.

Tornqvist, T.E., 1994. Middle and late Holocene avulsion history of the River Rhine (Rhine-Meuse Delta, Netherlands). Geology, 22: 711–714.

Welch, D.M., 1973. Channel form and bank erosion, Red River, Manitoba. Proc. Ninth Hydrology Symp., Edmonton, Alberta, Canada, pp. 284–293.

Wells, N.A. and Dorr, J.A., 1987. Shifting of the Kosi River, northern India. Geology, 15: 204–207.

Wilson, B.H., 1973. Some natural and man-made changes in the channels of the Okavango Delta. Botswana Notes Records, 5: 132–153.

Wilson, B.H. and Dincer, T., 1976. An introduction to the hydrology and hydrography of the Okavango Delta. Symp. on the Okavango Delta, Botswana Society, Gaborone, pp. 33–48.